J. Appl. Comput. Mech., 7(SI) (2021) 1252-1265
DOI: 10.22055/JACM.2020.32584.2039

ISSN: 2383-4536
jacm.scu.ac.ir

Shahid Chamran University of Ahvaz

Journal of Applied and Computational Mechanics

Research Paper

Validation of Model-Based Real-Time Hybrid Simulation for a Lightly-Damped and Highly-Nonlinear Structural System

Amirali Najafi[1], Billie F. Spencer Jr.[2]

[1] Department of Civil and Environmental Engineering, University of Illinois at Urbana-Champaign, Urbana, IL, 61801, USA, Email: anajafi2@illinois.edu

[2] Department of Civil and Environmental Engineering, University of Illinois at Urbana-Champaign, Urbana, IL, 61801, USA, Email: bfs@illinois.edu

Received February 11 2020; Revised March 09 2020; Accepted for publication March 16 2020.
Corresponding author: A. Najafi (anajafi2@illinois.edu)

Abstract. Hybrid simulation (HS) is a cost-effective alternative to shake table testing for evaluating the seismic performance of structures. HS structures are partitioned into linked physical and numerical substructures, with actuators and sensors providing the means for the interaction. Load application in conventional HS is conducted at slow rates and is sufficient when material rate-effects are negligible. Real-time hybrid simulation (RTHS) is a variation of the HS method, where no time-scaling is applied. Despite the recent strides made in RTHS research, the body of literature validating the performance of RTHS, compared to shake table testing, remains limited. In the few available studies, the tested structures and assemblies are linear or modestly nonlinear, and artificial damping is added to the numerical substructure to ensure convergence and stable execution of the simulation. The objective of this study is the validation of a recently proposed model-based RTHS framework, focusing on lightly-damped and highly-nonlinear structural systems; such structures are particularly challenging to consider using RTHS. The boundary condition in the RTHS tests are enforced via displacement and acceleration tracking. The modified Model-Based Control (mMBC) compensator is employed for the tracking action. A two-story steel frame structure with a roof-level track nonlinear energy sink (NES) device is selected due to its light damping, high nonlinearity, and repeatability. The complete structure is first tested on a shaking table, and then substructured and tested via the RTHS method. The model-based RTHS approach is shown to perform similar to the shake table method, even for lightly-damped and highly-nonlinear structures.

Keywords: RTHS validation; Shake table testing; Model-based control; Light damping; Nonlinear energy sink device.

1. Introduction

Shake table testing has historically been the primary method for assessment of structural performance under earthquake loading. Shaking tables are available in a variety of sizes and can test small- to full-scale structures. Extrapolation of structural performance from small-scale shake table tests requires detailed analysis of similitude laws on the materials, geometry, and test time scale, which is a complicated task. Shaking tables that can accommodate large-scale structures are also few, and expensive to operate.

The pseudo-dynamic or hybrid simulation (HS) method was introduced by Hakuno *et al.* [1], Takanashi *et al.* [2], and Mahin and Shing [3] as a means to overcome the limitations of the shake table testing. HS partitions structural systems into numerical and physical components. The physical partition is evaluated quasi-statically and restoring forces are measured and returned to the numerical model, which in turn solves the equation of motion for the next time step. Rate-dependent material effects which often result in larger failure capacities and smaller deformations are ignored, as a result of the application of forces over an extended time-scale [4]. Therefore, researchers have looked for alternative means for structural testing; namely methods with both substructuring and real-time capabilities.

Real-time hybrid simulation (RTHS) is an alternative to the traditional hybrid simulation, which offers the benefits of real-time testing (i.e., material rate-dependence can be accommodated) and substructuring (i.e., cost and space savings). With RTHS, physical execution happens in real-time and numerical integration is conducted explicitly at frequencies of 200 Hz or higher. Nakashima *et al.* [5] introduced the first example of RTHS, with an inner stabilizing loop running at 500 Hz, and a microcontroller solving the equation of motion at 50 Hz. Testing of a structure with a viscous damper was used to demonstrated RTHS capabilities. Dimig *et al.* [6] introduced the effective force testing method for RTHS, where for some given structural mass and ground motion, the experimental forces can be applied directly on the test structure. Force control is very sensitive to nonlinearities that exist in the dynamics of the servo-valve and actuators therefore, most adaptations of the RTHS method have been via displacement control, due to its stability and ease of implementation.

One of the challenges in RTHS is that researchers set higher than realistic (artificial) damping values to the numerical substructure to achieve stable execution. The execution of a successful experiment is often jeopardized by the presence of unwanted actuator-structure dynamics, which offset the amplitude and phase of the achieved signals in the physical execution.

Published online: March 31 2020

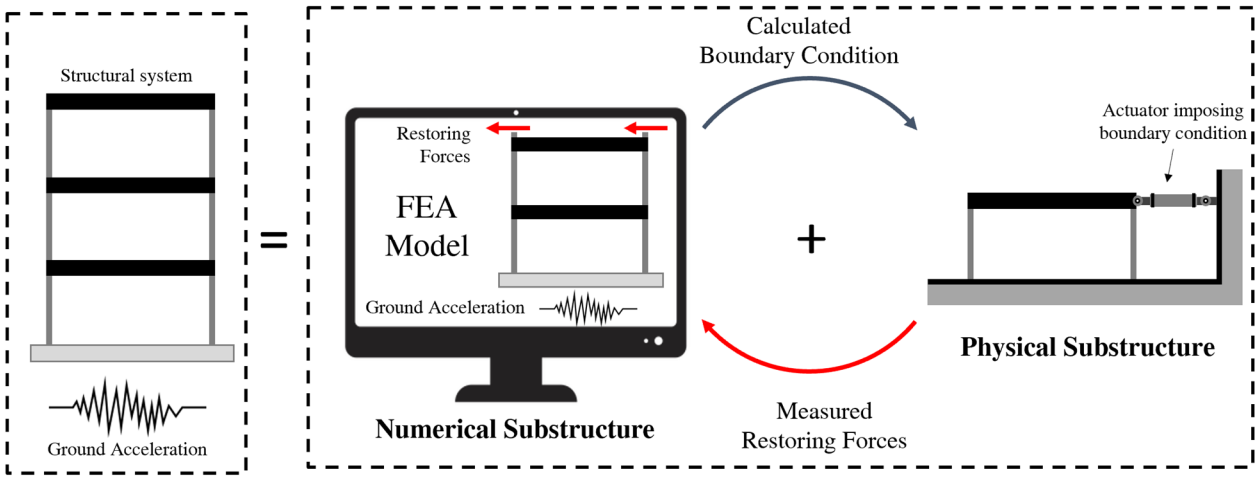

Fig. 1. Schematic illustration of the RTHS method

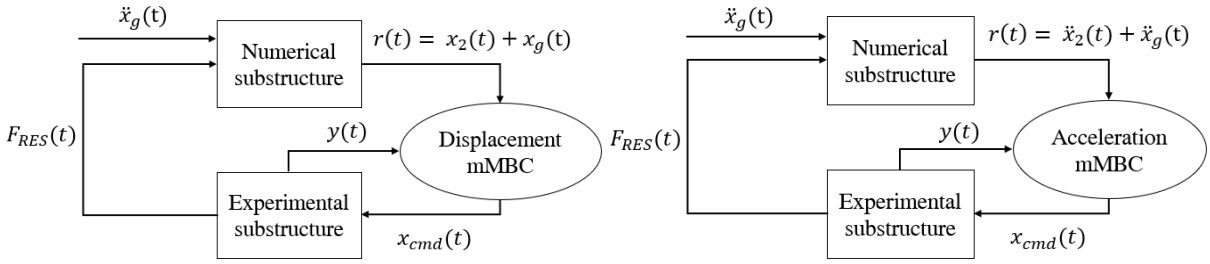

(a) RTHS with displacement tracking control

(b) RTHS with acceleration tracking control

Fig. 2. Model-based RTHS architecture

Horiuchi *et al.* [7] describes the effect of actuator phase delay as negative damping, which can jeopardize the stability of the RTHS experiment. Many researchers have thus used artificially high damping ratios ($\zeta > 5\%$) in the numerical substructure to enhance the stability of the RTHS. For example, Blakeborough *et al.* [8] discusses a two degree-of-freedom (DOF) experiment, where stability is achieved by setting a critical damping ratio of 5%. Nakata and Stehman [9] conducts RTHS on a multi-story building structure with damping ratios of 9.2%, 27.2%, and 43.9%, for the first three vibration modes. Shao *et al.* [10] presents a multi-story building with damping ratios of 6.9%, 7.4%, and 8.8%, for the first three vibration modes. However, as-built structures will not have such high damping. In a lightly-damped structural system where the negative damping associated with the closed-loop RTHS delays are significant, experiments may encounter loss of stability.

Model-based RTHS eliminates the need for the added artificial damping and results in a stable performance. This RTHS formulation addresses the challenge of unwanted actuator-structure dynamics via model-based compensation methods. Carrion and Spencer [11], Phillips and Spencer [12], and Chen *et al.* [13] proposed model-based compensation strategies for RTHS of magnetorheological (MR) damping devices. Model-based RTHS with acceleration tracking control was found to be suitable for acceleration sensitive physical substructures, as described by Zhang *et al.* [14]. Fermandois and Spencer [15] and Najafi *et al.* [16] applied the model-based approach to Load and Boundary Condition Boxes (LBCBs) at the University of Illinois at Urbana-Champaign in a multi-axial RTHS. Najafi and Spencer [17] presented an adaptive model reference augmentation to the model-based controller, to address the uncertainties in the RTHS control benchmark problem described by Silva *et al.* [18].

Another challenge with RTHS has surrounded the question of how the accuracy of this method is assessed. A number of publications in the recent years have investigated and compared the performances of shake table and various RTHS methods, as a means to validate the latter. Ashasi-Sorkhabi *et al.* [19] studied the dynamic performance of a spring-mass system coupled to a tuned liquid damper. The displacement response of the full- and sub-structured test configurations were evaluated and demonstrated to be closely matching. Damping of the analytical substructure was set to a high value of 6.3%. Lamarche *et al.* [20] conducted shake table and RTHS testing of a two-story reinforced concrete frame. Similar results were observed in the displacement response for the shake table and RTHS tests in both the linear- and nonlinear-range. However, validated methods for testing lightly-damped and highly-nonlinear structures don't appear to be available.

This paper investigates the potential of a recently proposed model-based RTHS method for testing lightly-damped and highly-nonlinear structural systems. The proposed model-based algorithm is comprised of substructuring the problem into numerical and physical components, with actuators imposing desired boundary conditions. The *modified model-based controller* (mMBC), introduced in Najafi and Spencer [21], is utilized for the tracking action of the boundary conditions. The shake table testing method is selected as a benchmark and used for validation of the proposed model-based RTHS. An illustrative example comprised of a reference two-story steel frame structure with a nonlinear energy sink (NES) device on the roof level is next introduced, due to its inherently low damping, high nonlinearity, and repeatability. First, the performance of the entire structure is evaluated via the shake table method. The two-story frame is then identified via a frequency-domain curve fitting method to estimate the parameters of the governing equations of motion (EOM). Next, RTHS experiments are conducted by physically testing the NES device and modeling the remainder of the structure numerically. Model-based RTHS is executed via both: (i) displacement tracking control, and (ii) acceleration tracking control of the boundary condition. Tracking via acceleration control is found to be more suitable for acceleration sensitive physical substructures. The responses of the first and second story displacements and accelerations are evaluated between the shake table and RTHS experiments. The comparison indicates that the model-based RTHS method can accurately replicate the results observed from the shake table tests for lightly-damped, highly-nonlinear structures.

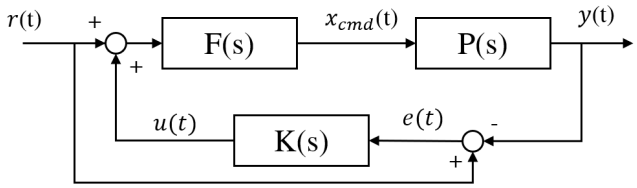

Fig. 3. Modified Model-Based Controller

Fig. 4. Two-story steel frame with track NES

Fig. 5. NES device

2. Model-Based RTHS Framework

The primary aim in this work is to validate the model-based RTHS method via comparison with shake table testing. Under the RTHS method, a structural system is partitioned into numerical and physical substructures per Fig. 1. The numerical model calculates the boundary condition motion with the physical substructure. Upon execution of boundary conditions via actuators, restoring forces are measured and returned to the numerical substructure. The model-based RTHS presented herein employs the modified Model-Based Controller (mMBC) developed by Najafi and Spencer [21], which has excellent tracking and robustness capabilities, making it a suitable controller for RTHS applications. Two types of model-based compensation are considered: 1) displacement tracking, and 2) acceleration tracking, as shown in Fig. 2. For completeness, this section provides a brief summary of the mMBC RTHS framework.

The mMBC compensation algorithm adopted for this paper is schematically shown in Fig. 3. The target and measured signals, $\boldsymbol{r}(t)$ and $\boldsymbol{y}(t)$ respectively, are displacement signals under displacement tracking control and acceleration signals under acceleration tracking control.

For a nominal linearized time-invariant actuator-structure dynamics $\mathbf{P}(s)$, a feedforward controller $\mathbf{F}(s)$, expressed in Laplace domain is defined as:

$$\mathbf{F}(s) = \mathbf{P}^{-1}(s)\mathbf{L}(s) \tag{1}$$

where $\mathbf{L}(s)$ is a lowpass filter. The lowpass filter is designed to ensure a proper realization for the feedforward controller, through the inclusion of appropriate number of poles. This filter also serves to attenuate high-frequency noise content.

The feedback control in the mMBC compensator is defined as linear-quadratic-gaussian (LQG) regulator which minimizes a quadratic cost function. The inputs to the cost function are the error signal $e(t)$, and feedback output signal $u(t)$, demonstrated in Fig. 3. The LQG cost function J_{LQG} is given by:

$$J_{LQG} = \mathbb{E}\left\{\int_0^\infty \left\{u^T R u + e^T Q e\right\} dt\right\} \tag{2}$$

$$u(s) = -\mathbf{K}(s)e(s) \tag{3}$$

where $\mathbb{E}$ is the expected value, R and Q are the weighting parameters for the cost function. For a stochastic system with Gaussi an process and observation noise, the design of the feedback controller is separated into a linear quadratic estimator (LQE) and a l inear quadratic regulator (LQR). The feedback controller $\mathbf{K}(s)$ is thus made up of an LQE and an LQR elements. The feedback contr oller is designed based on the combined action of the inverse model, lowpass filter, and the nominal plant model.

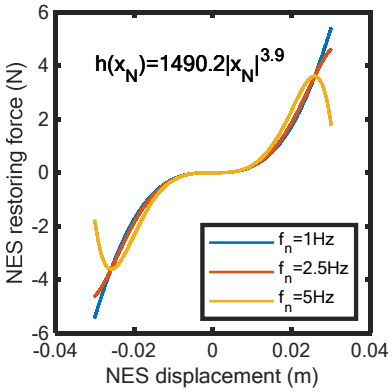

Fig. 6. Track NES hysteretic relationship for different excitation frequencies

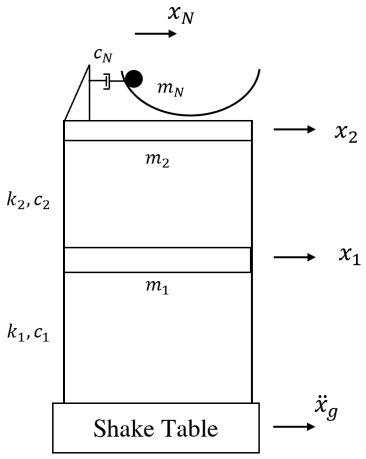

Fig. 7. Shake table testing: two-story steel frame with a track NES device

3. Selection of Structural Model

With the objective of conducting model-based RTHS on a structural system with light damping and high degree of nonlinearity, the next step is the selection of a structural model that meets these criteria. A two-story steel frame with a roof-level track nonlinear energy sink (NES) device, shown in Figs. 3 and 4, is selected. This two-story structure was previously studied in Wang *et al.* [22]. The two-story frame behaves as a shear building, because the floor slabs are considerably stiffer than the column sections. The structure is lightly damped, possessing a damping ratio of 0.20% and 0.36% for modes 1 and 2, respectively, when the NES is locked, and damping ratios of 0.45% and 0.38% when the NES is unlocked.

The NES mass moves along a vertically nonlinear path described by the shape of the track: $h(x_N)$, where x_N is the horizontal displacement of the mass. Fig. 5 describes demonstrates the track NES. Due to this geometric nonlinearity, the restoring forces of the NES are identified per the nonlinear equation below and shown in Fig. 6.

$$\Gamma = ([h'(x_N)]^2 \ddot{x}_N + h'(x_N)h''(x_N)\dot{x}_N + h(x_N))m_N \tag{4}$$

The two-story steel frame along with the track NES are modeled via three-DOF governing equations of motion with a ground acceleration as the input excitation, given by:

$$m_1\ddot{x}_1 + c_1\dot{x}_1 + c_2(\dot{x}_1 - \dot{x}_2) + k_1x_1 + k_2(x_1 - x_2) = -m_1\ddot{x}_g \tag{5}$$

$$m_2\ddot{x}_2 + c_2(\dot{x}_2 - \dot{x}_1) + k_2(x_2 - x_1) - c_N\dot{x}_N - \Gamma(t) = -m_2\ddot{x}_g \tag{6}$$

$$m_N\ddot{x}_N + c_N\dot{x}_N + \Gamma(t) = -m_N(\ddot{x}_2 + \ddot{x}_g) \tag{7}$$

where m_i, c_i, and k_i are mass, damping, and stiffness parameters, $\ddot{x}_i$, $\dot{x}_i$, and x_i are relative acceleration, velocity, and displacement terms of the i^{th} story, and c_N is the damping of the NES. m_N is the mass of the NES at 2.457 kg. $\ddot{x}_N$ and $\dot{x}_N$ describe the acceleration and velocity motions of the NES relative to the second-floor motion. $\ddot{x}_g$ is the ground acceleration. The schematic of the numerical realization of the two-story frame with the track NES device is shown in Fig. 7.

4. Shake Table Testing Result

The selected two-story steel frame with onboard track NES device is shake table tested in this section, as a benchmark for comparison with RTHS results in later sections. First, the physical hardware used are discussed including sensors used for motion detection. Next, the results of several shake tables tests are presented.

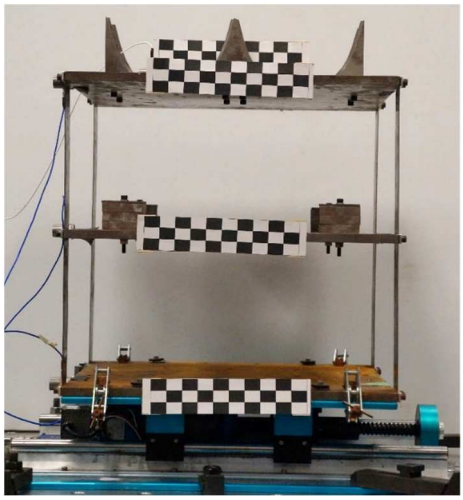

Fig. 8. Two-story steel frame with track NES device

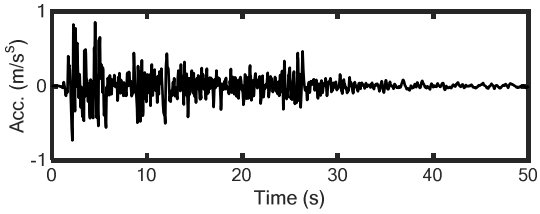

Fig. 9. 30% PGA-scaled 1940 El Centro earthquake

4.1 Experimental Hardware

The proposed experimental study is conducted on a Quanser Shake Table II. The DC motor onboard this shake table is powered with a Kollmorgen Silverline H-344-H-0600 amplifier. An NI CompactRIO 9073 controller completes the task of stabilizing the shake table via a proportional-derivative controller. Numerical integration and compensation action are computed on a dSPACE DS1103PPC microcontroller with a sampling rate of 1kHz. A 4th order Runge-Kutta integration algorithm is used. The development environment for the dSPACE controller consists of the Matlab/Simulink software suite and the ControlDesk program which converts algorithms to the C programming language and compiles them on the microcontroller.

4.2 Displacement and Acceleration Measurements

Measurement of the horizontal displacements at the story levels in the discussed steel frame is a challenging task. Linear displacement measurement tools like linear variable differential transformers (LVDTs) possess small amounts of friction, which can offset experimental results. To solve this issue, vision-based displacement measurement techniques are incorporated.

A 60 frame-per-second camera is used to record the behavior of the building during the duration of a ground motion acceleration. Black and white square patterns are installed on the structural components for detection via a vision-based algorithm, per in Fig. 8. Base (i.e., shake table) displacement is measured via the onboard optical encoder.

PCB 353B33 piezoelectric accelerometers are used for acceleration measurements. The accelerometers are installed at each story, on the NES, and on the shake table for acceleration feedback and compensation purposes. Following the data acquisition from the shake table testing procedure, results are synchronized and prepared for the model-based RTHS validation study.

4.3 Shake Table Results

The two-story steel frame with the track NES device is excited with a PGA-scaled 30% 1940 El Centro earthquake, shown in Fig. 9. This original ground acceleration was sampled at a 100 Hz from recording station no. 6, was upsampled to 1000 Hz for this study. The mMBC is used for compensation during the shake table testing and provides better tracking than many existing methods. Details pertaining to tracking control and operation of the shake table and two-story steel frame are presented in Najafi and Spencer [21].

Nonlinearities in the dynamics of the shake table device result in small performance variations in every experiment. These variations are presented in Fig. 10, along with the minimum and maximum values. To study these variations, results for 10 experiments are presented. Next, the structure is partitioned and tested via the RTHS method.

5. Real-Time Substructuring

Before conducting RTHS in the laboratory, the structure of interest is substructured and a numerical model identified. To this end, the two-story frame structure is partitioned into two substructures. The two-story frame is numerically modeled while the NES device is physically tested. The proposed RTHS substructuring is demonstrated in Fig. 11.

$$\begin{bmatrix} m_1 & 0 \\ 0 & m_2 \end{bmatrix}\begin{Bmatrix} \ddot{x}_1 \\ \ddot{x}_2 \end{Bmatrix} + \begin{bmatrix} c_1+c_2 & -c_2 \\ -c_2 & c_2 \end{bmatrix}\begin{Bmatrix} \dot{x}_1 \\ \dot{x}_2 \end{Bmatrix} + \begin{bmatrix} k_1+k_2 & -k_2 \\ -k_2 & k_2 \end{bmatrix}\begin{Bmatrix} x_1 \\ x_2 \end{Bmatrix} = -\begin{bmatrix} m_1 & 0 \\ 0 & m_2 \end{bmatrix}\begin{Bmatrix} 1 \\ 1 \end{Bmatrix}\ddot{x}_g - \begin{Bmatrix} 0 \\ 1 \end{Bmatrix}F_{RES} \tag{8}$$

where F_{RES} is the hybrid simulation restoring force, estimated using the acceleration data from the track NES shown in Fig. 12, defined as:

$$F_{RES} = m_N \ddot{x}_{N,abs} = m_N(\ddot{x}_N + \ddot{x}_2 + \ddot{x}_g) \tag{9}$$

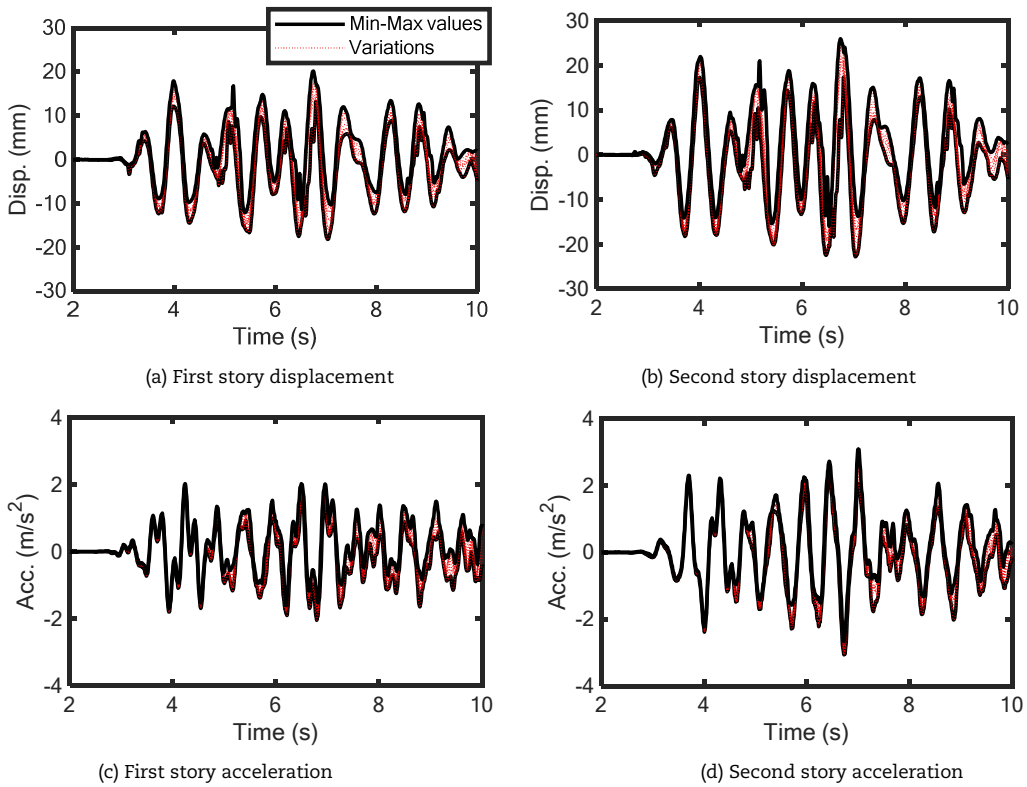

(a) First story displacement (b) Second story displacement

(c) First story acceleration (d) Second story acceleration

Fig. 10. Variations in the displacement and acceleration responses for 10 repeated shake table tests

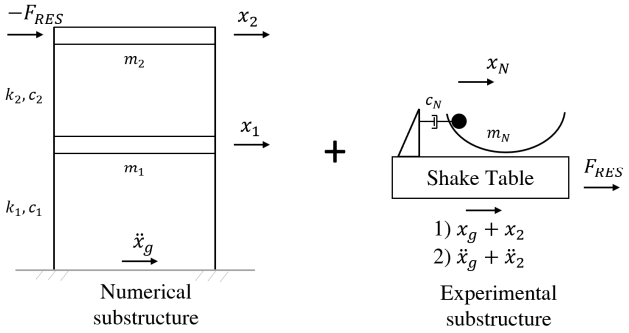

Fig. 11. RTHS testing: substructuring of the two-story frame with track NES

The two-DOF equation of motion of the two-story structure is next converted to state-space format for simulation purposes:

$$\begin{bmatrix}\dot{\mathbf{x}}_{Num}\\ \ddot{\mathbf{x}}_{Num}\end{bmatrix}=\begin{bmatrix}\mathbf{0} & \mathbf{I}\\ -\mathbf{M}^{-1}\mathbf{K} & -\mathbf{M}^{-1}\mathbf{C}\end{bmatrix}\begin{bmatrix}\mathbf{x}_{Num}\\ \dot{\mathbf{x}}_{Num}\end{bmatrix}+\mathbf{B}\ddot{x}_g+\mathbf{G}F_{RES} \tag{10}$$

$$y_1=\begin{bmatrix}0 & 1 & 0 & 0\end{bmatrix}\begin{bmatrix}\mathbf{x}_{Num}\\ \dot{\mathbf{x}}_{Num}\end{bmatrix}+x_g \tag{11}$$

$$y_1=\begin{bmatrix}-\mathbf{M}^{-1}\mathbf{K}(:,2) & -\mathbf{M}^{-1}\mathbf{C}(:,2)\end{bmatrix}\begin{bmatrix}\mathbf{x}_{Num}\\ \dot{\mathbf{x}}_{Num}\end{bmatrix} \tag{12}$$

where $\mathbf{M}$, $\mathbf{C}$ and $\mathbf{K}$ are mass, damping and stiffness matrices of the two-story frame and $\mathbf{x}_{Num} = [x_1 \quad x_2]^T$. Also, the input vectors are described as $B = [0 \quad 0 \quad -1 \quad -1]^T$ and $G = [0 \quad 0 \quad -[0 \quad 1]^T M^{-T}]^T$. The outputs of the numerical substructure are described as y_1 and y_2, which represent the second-floor displacement and acceleration, respectively. y_1 and y_2 are *boundary conditions* with the physical substructure, which are used in displacement and acceleration control, respectively.

In the proposed model-based RTHS setup, the boundary condition between the numerical and physical components is defined by the absolute motion of the second floor. A shake table is used to actuate the physical substructure. By replicating the absolute motion of the second floor, the shake table ensures that the NES device undergoes the same inertial forces, as it would if the complete structure was tested. Actuator compensation is provided in the form of the mMBC for displacement and acceleration control as discussed in section 2.

The physics of the NES mass is largely determined by the inertial behavior of this device, as stiffness and damping properties are insignificant. Since inertial behavior is directly proportional to the acceleration of the mass, it makes sense to control the acceleration behavior of the boundary condition, in order to ensure an accurate RTHS experiment.

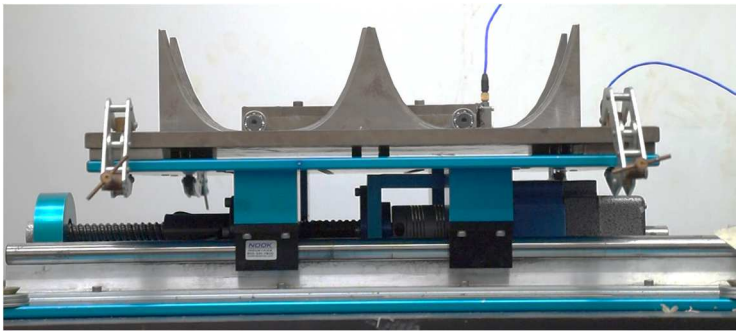

Fig. 12. RTHS physical substructure (NES mass)

5.1 Identifying the numerical model: two-story frame

A high-fidelity model of the two-story steel frame is next obtained via extraction of natural frequencies and mode shapes, and a particle swarm optimization (PSO) algorithm for model parameter optimization. The two-story frame structure (i.e., without the NES device), is installed on a shake table and excited with a BLWN voltage signal. Acceleration responses of the stories are recorded during this excitation. Time- and frequency-domain relationships between the input BLWN signal and recorded floor accelerations are used for the model identification. The process for modeling of the two-story steel frame involves the two steps: (i) parameter estimation, and (ii) parameter optimization.

5.1.1 Parameter Estimation

The first steps for reasonably accurate parameter estimations are listed below:

1. Estimate the story masses and formulate mass matrix, $\mathbf{M}$.
2. Identify the natural frequencies $\boldsymbol{\Omega} = \begin{bmatrix} \omega_1 & \omega_2 \end{bmatrix}^T$, via a peak-picking strategy.
3. Use the FRF phase relationships to estimate the mode shapes, $\boldsymbol{\Phi} = \begin{bmatrix} \boldsymbol{\Phi}_1 & \boldsymbol{\Phi}_2 \end{bmatrix}$.
4. Calculate the diagonal modal mass and stiffness matrices, $\hat{\mathbf{K}} = \left\{ \hat{k}_1, \hat{k}_2 \right\}$ and $\hat{\mathbf{M}} = \boldsymbol{\Phi}^T M \boldsymbol{\Phi} = \left\{ \hat{m}_1, \hat{m}_2 \right\}$, via $\hat{k}_i = \hat{m}_i \omega_i^2$ for $i \in \{1,2\}$.
5. Convert the stiffness matrix from modal to general stiffness coordinates, $\mathbf{K}$.

$$\mathbf{K} = \boldsymbol{\Phi}^{-T} \hat{\mathbf{K}} \boldsymbol{\Phi}^{-1} \tag{13}$$

6. Estimate the modal damping ratios ζ_i, for $i \in \{1,2\}$, by fitting the model to the peaks of the FRF plots.

5.1.2 Parameter Optimization

In the next step, the parameter estimates identified earlier are optimized, such that the numerical model of the two-story frame more accurately resembles the real physical performance. PSO uses a nature-inspired swarming strategy (i.e., bird flocking) and uses primitive mathematical operators to create an inexpensive computational tool [23]. Optimizing a structural model requires evaluation of multiple parameters. The evolutionary programming of the PSO algorithm is suitable for handling such a combinatorial optimization problem.

The PSO model begins by assigning a swarm of a particles to each optimization variable. A population of d random particles with a uniform distribution between the two boundaries b_l and b_h, and a position $x_{i,j} \sim U(b_l, b_h)$, and a velocity $v_{i,j}$ for $v_{i,j}$ $i \in \{1,\ldots,d\}$, where j is iteration count, are at first initialized for each variable. For the proposed structural model in eq. (8), the optimization variables are selected as k_1, k_2, m_1, m_2, ζ_1 and ζ_2. Each particle moves iteratively in the search-space and remembers its own optimal position P_i^L. The best position amongst all swarm particles are next stored in P_i^G. During each iteration, the velocity is updated per:

$$v_{i,j+1} = IT_j + CT_j + ST_j \tag{14}$$

$$IT_j = w v_{i,j} \tag{15}$$

$$CT_j = c_1 r_1 (P_i^L - x_{i,j}) \tag{16}$$

$$ST_j = c_2 r_2 (P_i^G - x_{i,j}) \tag{17}$$

where IT_j is an inertial term, CT_j is a cognitive term, and ST_j is a social term. r_1 and r_2 are uniformly distributed rand om vectors in $\sim U(0,1)$. w is the inertial weight, c_1 is the self-adjustment weight and c_2 is the social-adjustment weight. T he new position for each iteration is determined per below:

$$x_{i,j+1} = x_{i,j} + v_{i,j+1} \tag{18}$$

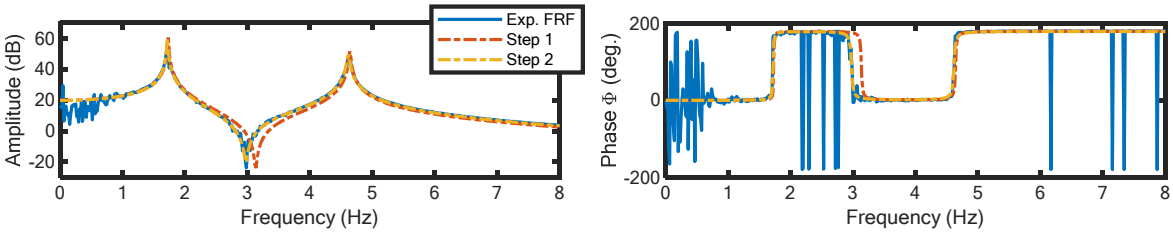

(a) Amplitude (b) Phase

Fig. 13. First story acceleration FRF

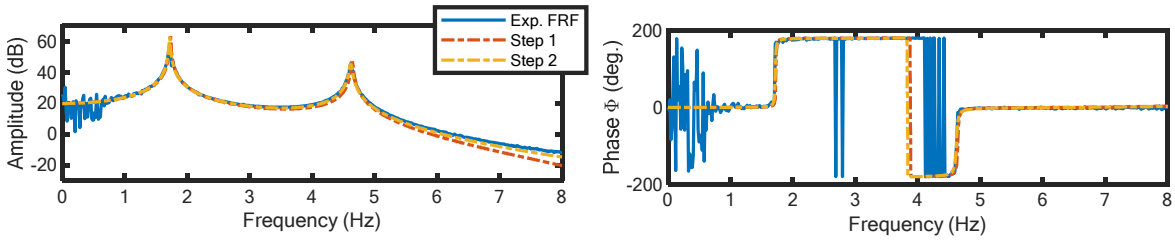

(a) Amplitude (b) Phase

Fig. 14. Second story acceleration FRF

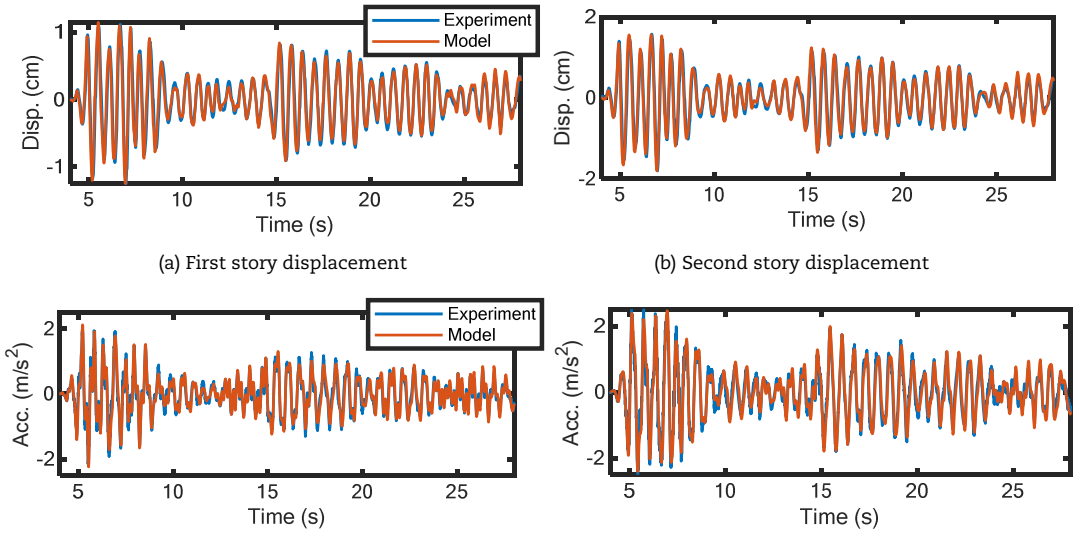

(a) First story displacement (b) Second story displacement

(c) First story acceleration (d) Second story acceleration

Fig. 15. Time-domain responses of the two-story structure – experimental and numerical results

Therefore, a particle can optimize its course based on the past experiences of itself and other swarm particles. The standard deviation (*SD*) between the measured and numerically computed first and second story accelerations, $a_{\exp}$ and a_{num} are used to develop the cost function in this optimization algorithm. Minimizing this cost function results in a reduction of errors between measured and numerically calculated accelerations. The SD is formulated per:

$$SD = \sqrt{\frac{\sum_{k=1}^{n}\left(a_{\exp}(k) - a_{num}(k)\right)^2}{n}} \tag{19}$$

where n is the data point count.

5.2 Two-story steel frame model

The parameters of the two-DOF system described in eq. (8) are next identified via the two-step process. The experimentally identified FRFs and fitted numerical models of the first and second story accelerations are shown in Fig. 13 and 14. The PSO in step 2 assists in improving the accuracy of the structural model.

The acceleration and displacement responses of the numerical model subjected to the El Centro 30% earthquake and are compared with the experimental results in Fig. 15.

The PSO algorithm is initialized with $d = 200$ swarm particles for each of the 6 structural parameters. Table 1 presents the predicted structural parameters after the estimation and optimization steps. This table also presents the lower and upper boundary values for the initialization of the swarm particles. The evolution of the swarm particles is demonstrated in Fig. 16, over the course of 15 iterations. These particles rarely converge to a single value due to the presence of an inertial term which ensures that their velocity is never converged to zero. Nevertheless, the position with the most optimized cost function is recorded and used.

Table 1. Identified parameters for two-story steel frame

Parameters	Step 1 (Parameter estimation)	b_l	b_h	Step 2 (Parameter optimization)
$m_1\ (kg)$	25.1	22.5	27.5	24.98
$m_2\ (kg)$	23.4	20.7	25.3	24.31
$k_1\ (N/m)$	7100	6390	7810	7238
$k_2\ (N/m)$	8300	7470	9130	8236
$\zeta_1\ (\%)$	0.250	0	1	0.196
$\zeta_2\ (\%)$	0.250	0	1	0.359

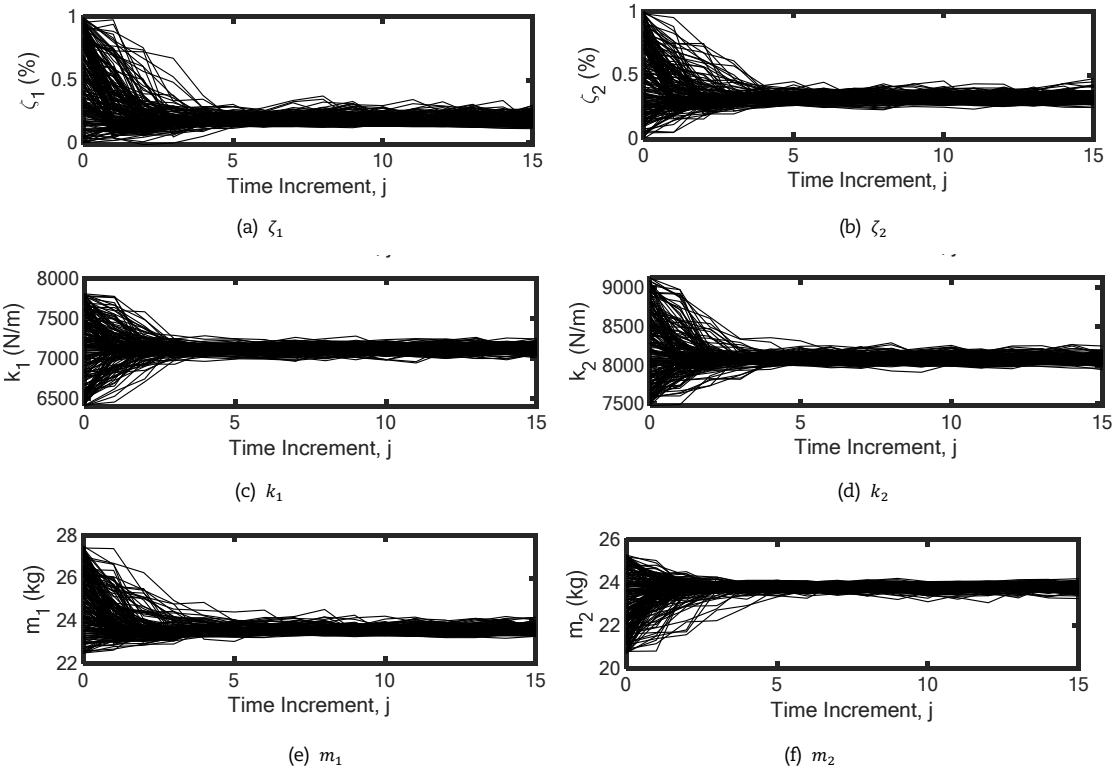

Fig. 16. Evolution of the swarm particles assigned to each variable

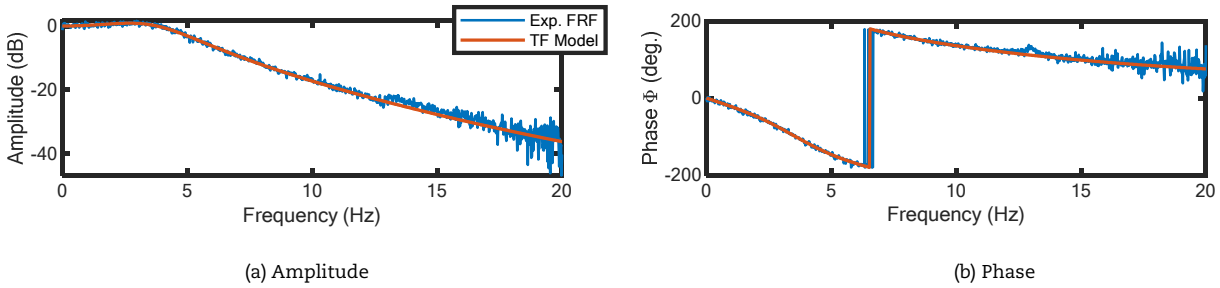

Fig. 17. $\mathbf{P}_{dd}(s)$ transfer system

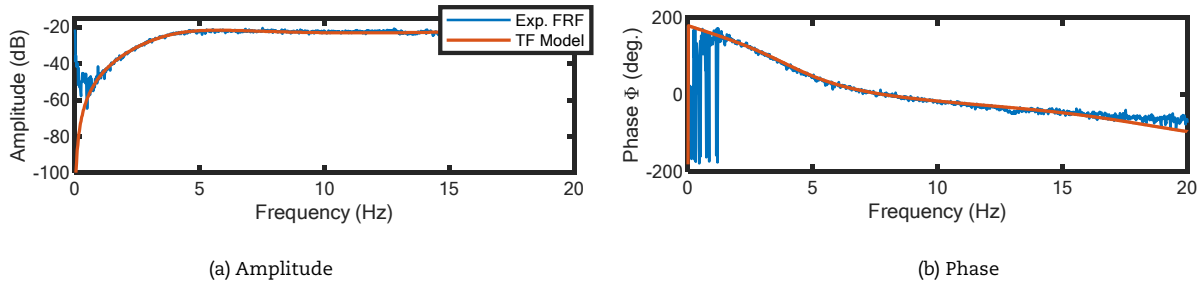

Fig. 18. $\mathbf{P}_{da}(s)$ transfer system

Table 2. Tracking performance error indices

Control type	Error index	
	PAE	RMSE
Displacement	3.649 (mm)	5.760 (mm)
Acceleration	0.938 (m/s^2)	0.667 (m/s^2)

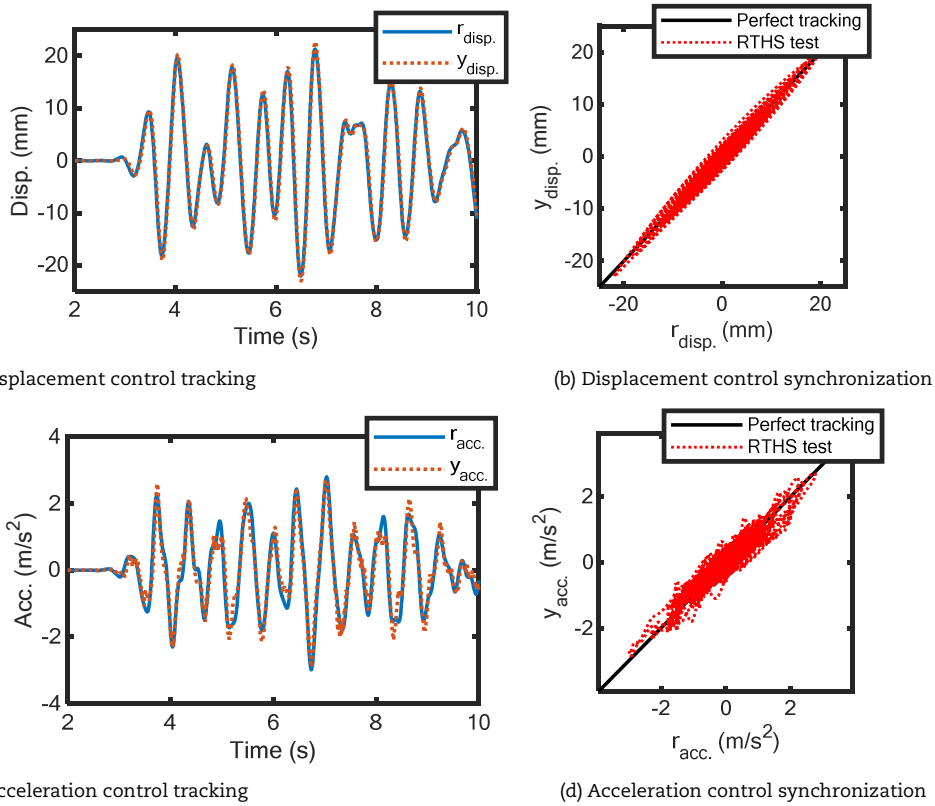

(a) Displacement control tracking

(b) Displacement control synchronization

(c) Acceleration control tracking

(d) Acceleration control synchronization

Fig. 19. Tracking and synchronization plots of the proposed mMBC compensator

5.3 Shake Table System Identification

The mMBC is developed using a linearized transfer function model of the shake table and structural system. The process for system identification, and frequency response function fitting are described in Najafi and Spencer [21]. Transfer function models of the shake table-structure interaction are used in the development of feedforward and feedback controllers.

System identification is conducted on the experimental substructure, which includes the shake table with the onboard NES device. A bandlimited gaussian white noise (BLWN) with a frequency range of 0 – 30Hz and an RMS amplitude of 0.2V is applied to the shake table and the realized displacements and accelerations are recorded.

Next, the time-domain results are transformed to frequency-domain to obtain frequency response functions (FRFs) for: (i) target displacement – measured displacement $\mathbf{P}_{dd}(s)$, and (ii) target displacement – measured acceleration $\mathbf{P}_{da}(s)$, transfer systems. The FRFs are fitted with transfer function models which are presented in Eqs. (20)-(21). The bode plot of the experimental FRFs and identified transfer models are shown in Fig. 17 and 18.

$$\mathbf{P}_{dd}(s) = \frac{d_{out}(s)}{d_{in}(s)} = \frac{4.67e6}{s^4 + 167s^3 + 1.14e4s^2 + 2.81e5s + 4.67e6} \tag{20}$$

$$\mathbf{P}_{da}(s) = \frac{a_{out}(s)}{d_{in}(s)} = \frac{1.18s^4 + 479.1s^3 + 4.83e4s^2}{s^4 + 126.6s^4 + 2.05e4s^3 + 1.09e6s^2 + 2.93e7s + 4.3e8} \tag{21}$$

The feedforward controller for displacement tracking is designed by cascading the inverse of the transfer system in eq. (20) with a fourth-order Butterworth lowpass filter with a cutoff frequency of 50 Hz. The feedforward controller for acceleration tracking is designed by cascading the inverse model of eq. (21) with first-order Butterworth lowpass filter with a cutoff frequency of 50 Hz.

5.4 mMBC RTHS Tracking Performance

Tracking performance results between the target and measured signals are evaluated for displacement control and acceleration control mMBC RTHS schemes. The time-histories of the target and measurement signals are presented in Fig. 19 (a) and (c). Tracking is qualitatively assessed via the synchronization plots in Fig. 19 (b) and (d). This x-axis displays the target signal and y-axis refers to the measured output signal. A 1:1 diagonal line indicates perfect tracking. However, since perfect tracking is difficult to achieve, even in the presence of a compensator, a more elliptic performance is obtained. Table 2 summarizes the Peak absolute error (PAE) and the root-mean-square error (RMSE) for the tracking performance of the proposed controller. These error indices are defined per:

$$PAE = \max\left|x_{meas}(k) - x_{t\,arg}(k)\right| \tag{22}$$

$$RMSE = \sqrt{\frac{\sum_{k=1}^{n}\left(x_{meas}(k) - x_{t\,arg}(k)\right)^2}{n}} \tag{23}$$

6. Shake Table and Model-Based RTHS Comparison

The performance and variations in the behavior of the two-story structure subject to a ground motion excitation are examined using both shake table testing and model-based RTHS in this section. The variables relevant to this study are the first and second story relative displacements and absolute accelerations. Particular attention is paid to the second story motions, as this floor formulates the boundary condition between the physical and numerical substructures.

6.1 mMBC RTHS tracking performance

Due to the nonlinear behavior of the actuator (i.e., shake table), variations exist in the performance of the RTHS experiments. Therefore, 10 experiments are conducted for the evaluation of the displacement control RTHS and another 10 for the acceleration control RTHS. The RTHS experiments are next compared to the 10 shake table tests conducted earlier. Every shake table and RTHS experiment is cross evaluated using the RMSE criterion and the results are displayed in the RMSE bar charts in Fig. 20 and 21.

Experimental results are post-processed through synchronization and low- and highpass filtering. In all experiments, the measured data are synchronized with their corresponding input ground motion. Since the ground motions are identical between all experiments, synchronization is conducted by matching the input ground motions. Next, measured data are post-processed with a second-order Butterworth lowpass filter with a cutoff frequency of 15 Hz, and a second-order Butterworth highpass filter with a cutoff frequency of 0.5 Hz.

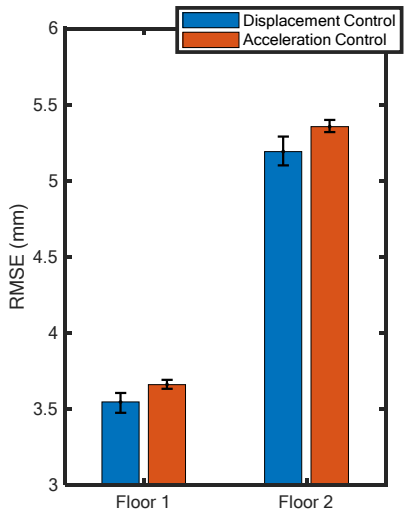

Fig. 20. RMSE median and interquartile range for displacement results

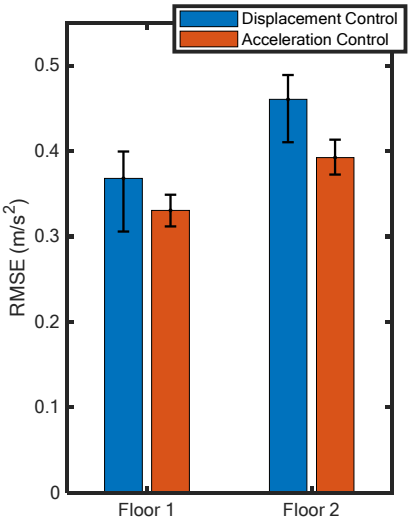

Fig. 21. RMSE median and interquartile range for acceleration results

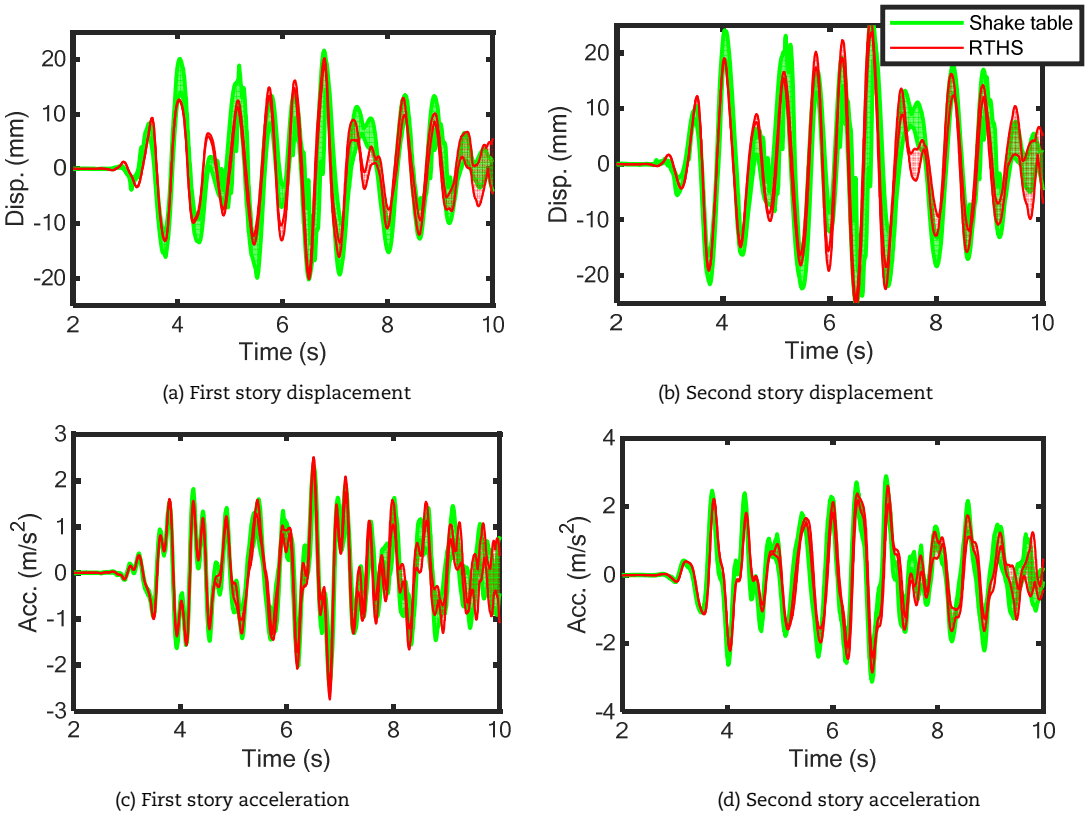

(a) First story displacement (b) Second story displacement

(c) First story acceleration (d) Second story acceleration

Fig. 22. Shake table and RTHS variational comparison – Displacement control

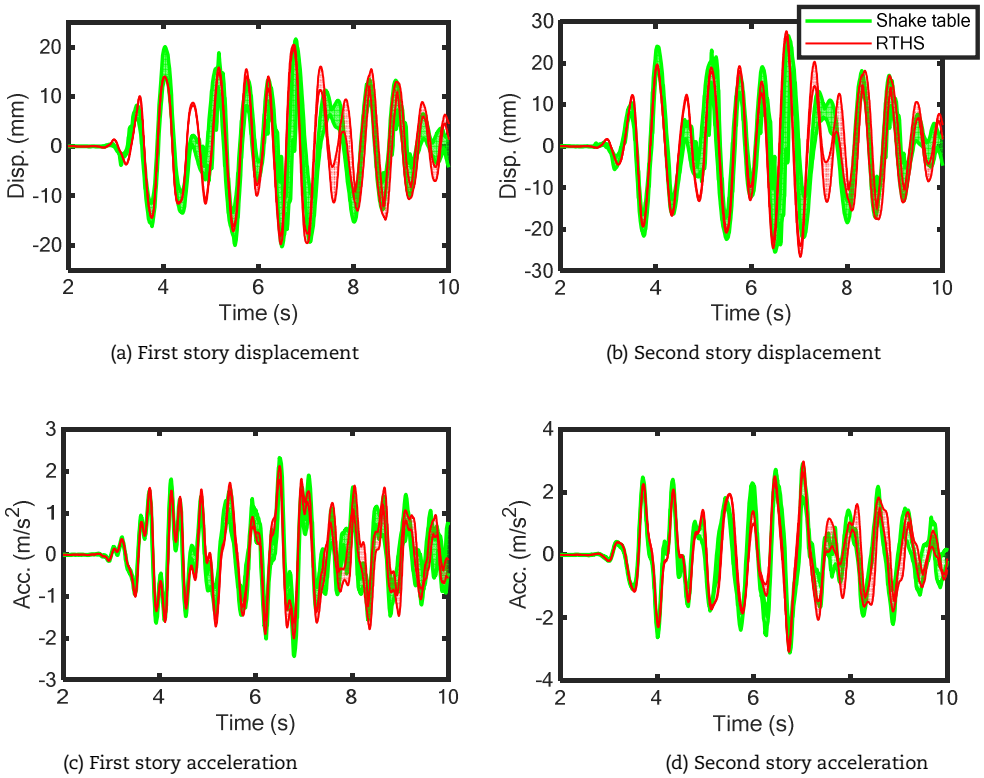

(a) First story displacement (b) Second story displacement

(c) First story acceleration (d) Second story acceleration

Fig. 23. Shake table and RTHS variational comparison – Acceleration control

7. Conclusion

The proposed study evaluates the performance of the model-based RTHS framework in comparison with the shake table testing method, for a lightly-damped, highly-nonlinear, and rate-dependent structure. The selected structure is comprised of a two-story steel frame and a nonlinear energy sink (NES) device on the roof level. Two model-based RTHS strategies involving displacement and acceleration tracking control of the boundary condition with the physical substructure are explored. The two-story steel frame is evaluated as the numerical substructure and the roof-level NES device is tested physical in the RTHS realization. A Quanser Shake Table II was used for the physical testing in this study. For the computation modeling of the two-story frame, a two-step system

identification procedure was proposed which included parameter estimation and optimization. Structural parameters, like stiffness, damping, and mass are estimated from the natural frequencies and mode shapes in the parameter estimation step, and then optimized via a PSO algorithm in the parameter optimization step. The modified model-based control (mMBC) algorithm was used for the compensation of the shake table-structure dynamics. This controller was implemented in both acceleration and displacement control. Upon execution of the control signal, restoring forces were estimated using the measured acceleration of the NES device and returned to the numerical model. The results indicate a good match between the structure performance with shake table and model-based RTHS tests.

Author Contributions

A. Najafi planned and conducted the conceptualization, methodology, software, investigation and analysis, data curation, and writing of the original draft; B.F. Spencer Jr. conducted the writing, review and editing, supervision and project administration. Both authors discussed the results, reviewed and approved the final version of the manuscript.

Conflict of Interest

The authors declared no potential conflicts of interest with respect to the research, authorship and publication of this article.

Funding

The authors received no financial support for the research, authorship and publication of this article.

References

[1] Hakuno, M., Shidawara, M., and Hara, T., Dynamic destructive test of a cantilever beam, controled by an analog-computer, *Trans. Japan Society of Civil Engineers*, 171, 1969, 1–9.
[2] Takanashi, K., Udagawa, K., Seki, M., Okada, T., and Tanaka, T., Non-linear earthquake response analysis of structures by a computer-actuator on-line system (details of the system), *Architectural Institute of Japan Transactions*, 229, 1975, 77–83.
[3] Mahin, S. A. and Shing, P. B., Pseudodynamic method for seismic testing, *Journal of Structural Engineering*, 111(7), 1985, 1482–1503.
[4] Saouma, V. *et al.*, Real-Time Hybrid Simulation of a Nonductile Reinforced Concrete Frame, *Journal of Structural Engineering*, 140(2), 2014, 1–12, doi: 10.1061/(ASCE)ST.
[5] Nakashima, M., Kato, H., and Takaoka, E., Development of real-time pseudo dynamic testing, *Earthquake Engineering and Structural Dynamics*, 21, 1992, 79–92.
[6] Dimig, J., Shield, C., French, C., Bailey, F., and Clark, A., Effective force testing: a method of seismic simulation for structural testing, *Journal of Structural Engineering*, 125(9), 1999, 1028–1037.
[7] Horiuchi, T., Nakagawa, M., Sugano, M., and Konno, T., Development of a Real-time Hybrid Experimental System with Actuator Delay Compensation, *Proc. of 11th World Conf. Earthquake Engineering*, 1996.
[8] Blakeborough, B. A., Williams, M. S., Darby, A. P., and Williams, D. M., The development of real-time substructure testing, *Philosophical Transactions of the Royal Society A Mathematical, Physical and Engineering Sciences*, 359, 2001, 1869–1891.
[9] Nakata, N. and Stehman, M., Compensation Techniques for Experimental Errors in Real-Time Hybrid Simulation Using Shake Tables, *Smart Structures and Systems*, 14(6), 2014, 1055–1079.
[10] Shao, X., Reinhorn, A. M., and Sivaselvan, M. V., Real-Time Hybrid Simulation Using Shake Tables and Dynamic Actuators, *Journal of Structural Engineering*, 137(7), 2011, 748–760.
[11] Carrion, J. E. and Spencer, B. F., *Model-based Strategies for Real-time Hybrid Testing*, NSEL Report Series, University of Illinois, Report No. NSEL-006, 2007.
[12] Phillips, B. M. and Spencer, B. F., Model-Based Multiactuator Control for Real-Time Hybrid Simulation, *Journal of Engineering Mechanics*, 139, 2013, 219–228.
[13] Chen, P.-C., Chang, C.-M., Spencer, B. F., and Tsai, K.-C., Adaptive model-based tracking control for real-time hybrid simulation, *Bulletin of Earthquake Engineering*, 13(6), 2015, 1633–1653.
[14] Zhang, R., Phillips, B. M., Taniguchi, S., Ikenaga, M., and Ikago, K., Shake table real-time hybrid simulation techniques for the performance evaluation of buildings with inter-story isolation, *Structural Control and Health Monitoring*, 24(10), 2017, 1–19.
[15] Fermandois, G. A. and Spencer, B. F., Model-based framework for multi-axial real-time hybrid simulation testing, *Earthquake Engineering and Engineering Vibration*, 16(4), 2017, 671–691.
[16] Najafi, A., Fermandois, G. A., and Spencer, Jr., B. F., Model-based real-time hybrid simulation with multi-axial load and boundary condition boxes, *Under review*, 2020.
[17] Najafi, A. and Spencer, B. F., Adaptive model reference control method for real-time hybrid simulation, *Mechanical Systems and Signal Processing*, 132, 2019, 183–193.
[18] Silva, C. E., Gomez, D., Maghareh, A., Dyke, S. J., and Spencer Jr., B. F., Benchmark control problem for real-time hybrid simulation, *Mechanical Systems and Signal Processing*, 135, 2020, 106381.
[19] Ashasi-Sorkhabi, A., Malekghasemi, H., and Mercan, O., Implementation and verification of real-time hybrid simulation (RTHS) using a shake table for research and education, *Journal of Vibration and Control*, 21(8), 2015, 1459–1472.
[20] Lamarche, C. P., Tremblay, R., Leger, P., Leclerc, M., and Bursi, O. S., Comparison between real-time dynamic substructuring and shake table testing techniques for nonlinear seismic applications, *Earthquake Engineering and Structural Dynamics*, 39, 2010, 1299–1320.
[21] Najafi, A. and Spencer, B. F., Modified model-based control of shake tables for online acceleration tracking, *Earthquake Engineering and Structural Dynamics*, 2020, https://doi.org/10.1002/eqe.3326.
[22] Wang, J., Wierschem, N. E., Spencer, B. F., and Lu, X., Experimental Study of Track Nonlinear Energy Sinks for Seismic Reduction, *The 5th Tongji-UBC symposium on Earthquake Engineering – Facing Earthquake Challenges Together*, Tongji University Shanghai, May 4-8, China, 2015..
[23] Kennedy, J. and Eberhart, R., Particle Swarm Optimization, in *Proceedings of the ICNN'05 - Internatinal Conference on Neural Networks*, 1995, 1942–1948.

ORCID iD

Amirali Najafi https://orcid.org/0000-0002-7845-0859
Billie F. Spencer Jr. https://orcid.org/0000-0003-0517-7908

How to cite this article: Najafi A., Spencer Jr. B.F. Validation of Model-Based Real-Time Hybrid Simulation for a Lightly-Damped and Highly-Nonlinear Structural System, *J. Appl. Comput. Mech.*, 7(SI), 2021, 1252–1265. https://doi.org/10.22055/JACM.2020.32584.2039